scientific reports

Check for updates

OPEN

Oxidative phosphorylation related gene COA6 is a novel indicator for the prognosis and immune response in lung adenocarcinoma

Wenting Liu[1,2,4], Yantao Jiang[1,4], Guoli Li[3,4], Dingzhi Huang[1]✉ & Tingting Qin[1]✉

Although the initial research focused on glycolysis, mitochondrial oxidative phosphorylation has become a major target of cancer cells. Cytochrome C oxidase assembly factor 6 (COA6) is a conserved assembly factor necessary for complex IV biogenesis. Nevertheless, the clinical predictive value of COA6, especially its correlation with immune cell infiltration in lung adenocarcinoma (LUAD), has not yet been elucidated. COA6 exhibited higher expression levels in LUAD cells and tumor tissues compared to normal tissues. Additionally, heightened COA6 expression was associated with reduced overall survival (OS) and advanced tumor stage. Apart from its role in mitochondrial respiratory processes, COA6 may be involved in the process of antigen binding, immunoglobulin receptor binding. Interestingly, we observed a positive correlation between COA6 expression and tumor mutational burden (TMB), as well as a significant association with decreased immune cell infiltration. COA6 was linked to resistance against gemcitabine and etoposide. We verified that COA6 was highly expressed in LUAD experimentally and cell proliferation was inhibited after COA6 knockdown. Thus, we conclude that the expression of COA6 was correlated with reduced immune cell infiltration. Additionally, COA6 functioned as a biomarker for drug sensitivity and the prognosis of lung adenocarcinoma.

Keywords Lung adenocarcinoma, COA6, Immune infiltration, Biomarker, Prognosis

Reprogramming energy metabolism has been accepted as the core hallmarks of cancer. Aerobic glycolysis is favored rather than oxidative phosphorylation (OXPHOS) in tumor cells. However, mitochondrial OXPHOS generates 17-fold more ATP relative to glycolysis. As reported, OXPHOS generated 80% of the adenosine triphosphate (ATP) demand of normal cells on average while 83% of the ATP demand of tumor cells[1]. It means OXPHOS remains playing an important role in energy contribution to cancers. The mitochondrial OXPHOS system consists of five multi-subunit protein complexes, including cytochrome C oxidase (complex IV; COX)[2]. COX is a complex at the end of the mitochondrial electron transport chain and catalyzes the reduction of molecular oxygen to water, thus contributing to the generation of proton motive force and complex V uses proton motive force to synthesize ATP[3,4]. Oncology agents targeting OXPHOS, including panhematin combined with metformin (complex I)[5], fenofibrate (complex I)[6], and arsenic trioxide (complex IV)[7], have been approved by the U.S. Food and Drug Administration for clinical use.

Lung cancer is the most common cancers worldwide and remains the leading cause of cancer-related death. In 2020, it was estimated that there were nearly 2.2 million new cases of lung cancer and approximately 1.8 million deaths attributed to the disease[8]. Non-small cell lung cancer (NSCLC) accounts for approximately 80–85% of lung cancer cases, with lung adenocarcinoma (LUAD) being the dominant subtype, accounting for 50% cases[9]. Despite notable advancements in targeted therapy and immunotherapy, the clinical outcomes for NSCLC patients remain unsatisfactory. Consequently, there is a critical need to explore new targets and gain fresh insights for the development of drugs to combat lung cancer.

Cytochrome C oxidase assembly factor 6 (COA6), also known as C1orf31, is a small protein located in intermembrane with a dual CX9C motif. The biogenesis of COX is a highly sophisticated process. COA6 is

[1]Department of Thoracic Oncology, Tianjin Key Laboratory of Cancer Prevention and Therapy, Tianjin Medical University Cancer Institute and Hospital, National Clinical Research Center for Cancer, Tianjin's Clinical Research Center for Cancer, Tianjin 300060, China. [2]Department of Respiratory Medicine, Beijing Friendship Hospital, Capital Medical University, Beijing 100050, China. [3]Department of Clinical Laboratory, Beijing Chao-Yang Hospital, Capital Medical University, Beijing 100020, China. [4]Wenting Liu, Yantao Jiang and Guoli Li contributed equally to this work. ✉email: dingzhih72@163.com; shadowzlyy@163.com

a conserved complex IV assembly factor necessary for COX2 subfundalization[10,11], which plays an important role in CuA biogenesis. Copper is critical for COX assembly, activity and stability. Loss of COA6 leads to severe COX loss in many organisms[11]. Moreover, loss of COA6 functional mutations in human mitochondrial disease leads to fatal infant cardiomyopathy, further highlighting its critical needs in cellular respiration[12,13]. Recent studies showed that COA6 was associated with the prognosis of hepatocellular carcinoma[14] and lung adenocarcinoma[15,16]. Nonetheless, it remains unclear whether the expression levels of COA6 are linked to the tumor infiltration of immune cells in patients with LUAD.

In this study, we validated the expression levels of COA6 in both LUAD cells and tissues through a combination of experimental and bioinformatics methods. Furthermore, our investigation established a relationship between elevated COA6 expression, clinicopathological outcomes, and the prognosis of LUAD patients. Lastly, we identified a notable correlation between elevated COA6 expression, reduced immune infiltration, and drug resistance. The findings of this study suggest that COA6 may impact the prognosis of LUAD patients via distinct pathways.

Materials and methods

Data sources

COA6 gene expression and corresponding clinical data were downloaded from The Cancer Genome Atlas (TCGA) (https://portal.gdc.cancer.gov/) and USUC XENA database (https://xenabrowser.net/datapages/). COA6 expression level, calculated as transcripts per kilobase million (TPM), were analyzed using R (version 4.2.1) and graphed with the ggplot2 (version 3.3.6) package. GSE31210 datasets from the Gene Expression Omnibus (GEO) (https://www.ncbi.nlm.nih.gov/geo/) database was also retrieved as validation cohort.

Expression profiles and prognostic value of COA6 on public platforms

mRNA expression of COA6 were compared between tumor and normal tissues across cancers using the GTEx-TCGA datasets. Expression differences of COA6 protein between LUAD tissues and normal lung tissues were compared by Cancer Proteogenomic Data Analysis Site (https://cprosite.ccr.cancer.gov). Part of IHC Figures were acquired from The Human Protein Atlas (HPA, https://www.proteinatlas.org/). The survival map of COA6 in across cancers was plotted using GEPIA2.0 (http://gepia2.cancer-pku.cn/#index). The relationship between clinical features and COA6 expression were analyzed using Mann-Whitney U test. Receiver operating characteristic (ROC) curve analysis were carried out using R with 'pROC' package. Survival analyses were performed using Kaplan-Meier estimation of overall survival (OS) by 'survival' package. Single-cell functional states data was obtained from CancerSEA (http://biocc.hrbmu.edu.cn/CancerSEA/).

Functional enrichment analysis

To explore the biological functions associated with COA6, 303 differentially expressed genes between low-and high-COA6 expression patients were identified using the 'limma' package with a criterion of $|\log FC| > 0.7$ and further used to performed Gene Ontology (GO) analyses, and Kyoto Encyclopedia of Genes and Genomes (KEGG)[17–19] enrichment analysis using R clusterProfiler package. To validate COA6 roles in LUAD, the Gene Set Enrichment Analysis (GSEA) was performed, and the top 8 terms were exhibited.

Protein–protein interaction (PPI) analysis

212 genes significantly correlated with COA6 were identified using pearson correlation analysis with the criteria $Cor > 0.4$ and generated the PPI network from the STRING (https://cn.string-db.org/) database. The most connected subnetworks were identified using the Cytoscape's Mcode plugin and their biological functions were visualized by the Cluego plugin.

Somatic mutation analysis

The somatic mutation data of LUAD patients were acquired from the TCGA database. The association of COA6 expression with correspondent TMB value was analyzed by pearson correlation test. The 'maftools' package was used to calculate tumor mutation burden of each LUAD patients and generated the mutation waterfall plots of low and high COA6 expression groups.

Immune infiltration and drug sensitivity analysis

The 'ESTIMATE' package was applied to compute the ESTIMATE, immune, stromal scores and tumor purity of each LUAD sample. To determine the types of tumor infiltration immune cells affected by COA6, we used single-sample GSEA (ssGSEA) algorithm with 'GSVA' package to evaluate the immune scores of 28 immune cells[20]. To access the correlation of COA6 with immune checkpoints, the Wilcoxon test was performed between low and high COA6 expression groups.

The TIDE algorithm was used to estimate the difference of low and high COA6 expression groups in benefiting from immunotherapy. The 'pRRophetic' algorithm was conducted to calculate the half-maximal inhibitory concentration (IC50) values of multiple common drugs. The difference of drug sensitivity between low and high COA6 expression patients was analyzed using Wilcoxon test and the correlation of IC50 values with COA6 expression was assessed using the spearman correlation coefficient.

Cell culture and construction of stably infected cell lines

The human NSCLC cell lines (A549 and PC-9), which were obtained from Cell Resource Center, Institute of Basic Medical Science CAMS/PUMC, were cultured in RPMI 1640 medium (Gibco, USA) with 10% fetal bovine serum (Zeta life, France) and penicillin-streptomycin solution (50 μg/mL). All cultures were maintained at 37 °C under humidified atmosphere containing 5% CO2.

Stable cell lines (A549-COA6-sh1, A549-COA6-sh2, PC-9-COA6-sh1, PC-9-COA6-sh2) were generated using lentiviral transduction. Lentivirus was generated in 293FT cells by transfecting the transfer plasmid (COA6-shRNA series) together with packaging plasmids PLP1, PLP2 and VSVG. COA6-shRNA plasmids were purchased from Public Protein/Plasmid Library using the pPLK vector.

Reverse transcription quantitative polymerase chain reaction (RT-qPCR)

We extracted total RNA from A549 and PC-9 cells using TRIzol reagent (Invitrogen, USA), and reverse transcribed total RNA into complementary DNA using PrimeScript™ RT reagent Kit (#RR420A, Takara, China). Subsequently, Universal Blue qPCR SYBR green Master Mix (Yeasen, China) was used for RT-qPCR. COA6 primers followed the 5' to 3' direction: ATCGCCTGCTTGGTGATTGTGG (forward) and GTTCTCATCTA AACACTTCCAGTAC (reverse) (CAT#: HP202276). We used GAPDH as the reference primer (Forward: G TCTCCTCTGACTTCAACAGCG; Reverse: ACCACCCTGTTGCTGTAGCCAA) (CAT#: HP205798). The experiment was repeated three times. The level of COA6 mRNA expression was calculated with the $2^{-\Delta\Delta Ct}$ method. Other primers are listed in the Supplementary Table 1.

Western blotting (WB)

Cells were lysed in RIPA buffer with 1mM PMSF and protease inhibitor cocktail. The COA6 protein concentrations were determined with bicinchoninic acid protein assay (Solarbio, PC0020). Protein samples were resolved by SDS-PAGE and subsequent transfer to PVDF membranes. After blocking, membranes were incubated with primary antibodies of COA6 (1:1000, Proteintech, Cat No. 24209-1-AP, China) or GAPDG (1: 1000, CTS, #2118, USA) at 4 °C overnight, followed by incubation with a corresponding second antibody (1: 5000, CST, USA). Blots were obtained by chemiluminescence with ECL substrate using Tanon 5200 chemiluminescence imaging system.

Immunohistochemistry staining (IHC)

We collected 40 LUAD tissues and 10 adjacent normal lung tissues from patients who underwent surgery between December 2012 and February 2014 at the Tianjin Cancer Institute and Hospital, which was approved by the Ethics Committee of the Tianjin Cancer Institute and Hospital (approval number: bc2023091) and in accordance with the Declaration of Helsinki. All patients had not received preoperative therapy and were pathologically diagnosed with LUAD.

Tumor tissues were fixed and embedded in paraffin. Tissue sections were deparaffinized and rehydrated with xylene and concentration gradient ethanol, respectively. Antigen retrieval was performed in antigen repair buffer by microwave. 3% hydrogen peroxide was used to inactivate endogenous peroxidase. Tissue sections were incubated with COA6 antibody (1:600) overnight. Then, tissue sections were washed with PBS buffer and incubated with antibody signal enhancer and secondary antibody. Subsequently, specimens were conjugated with HRP and Cardassian DAB Chromogen, followed by retained with hematoxylin and hydrated. The degree of immunostaining was measured by Image Pro Plus (version 6.0).

Cell proliferation

The stably transfected A549 and PC-9 were divided into different groups and seeded onto a 96-well plate at a density of 5×10^4 cells/ml. We used the MTT (Solarbio, China) to determine the proliferative capacity of cells. After 24, 48, 72 h, the medium was replaced with 100 μL of MTT solution (0.5 mg/mL in cell culture medium) and incubated at 37 °C for 4 hours. MTT solution was then removed, and MTT formazan was dissolved in 150 μL DMSO. Absorbance was read immediately in a microplate reader (BioTek, America) using a wavelength of 450 nm.

Additionally, the plate colony formation assay was performed to evaluate the colony formation ability of tumor cells. The stably transfected cells were seeded at decreasing densities in six-well plates, which was assessed with crystal violet staining after 14 days cell culture.

Cell cycle distribution was measured by cell cycle and apoptosis analysis kit (YEASEN, China) according to manufacturer's instructions. Samples were analyzed on the CytoFLEX LX flow cytometer (Beckman Coulter) and FlowJo v10.80 software.

Statistics analysis

R software (version 4.2.2) was used to perform statistical analysis. All statistical results with p-values < 0.05 were considered statistically significant (ns, $p \geq 0.05$; *, $p < 0.05$; **, $p < 0.01$; ***, $p < 0.001$). The association between continuous variables will be assessed using either independent samples t-test (normal distribution) or Mann-Whitney U test (skewed data), while the relationship between categorical variables will be analyzed using chi-square X^2 test or Fisher's exact test.

Results

Overexpression of COA6 in pan-cancers

COA6 expression was found relative higher in multiple cancers than normal tissues. We first assessed COA6 mRNA expression in 33 cancers via TCGA database, and overexpression of COA6 was discovered in 13 cancers compared with normal tissues: lung adenocarcinoma(LUAD), lung squamous cell carcinoma(LUSC), bladder urothelial carcinoma (BLCA), breast invasive carcinoma(BRCA), cervical squamous cell carcinoma and endocervical adenocarcinoma(CESC), cholangiocarcinoma(CHOL), colon adenocarcinoma(COAD), esophageal carcinoma(ESCA), head and neck squamous cell carcinoma(HNSC), liver hepatocellular carcinoma(LIHC), pancreatic adenocarcinoma(PAAD), stomach adenocarcinoma(STAD), and uterine corpus endometrial Carcinoma(UCEC) (Fig. 1a). Furthermore, overexpression of COA6 in LUAD, adrenocortical

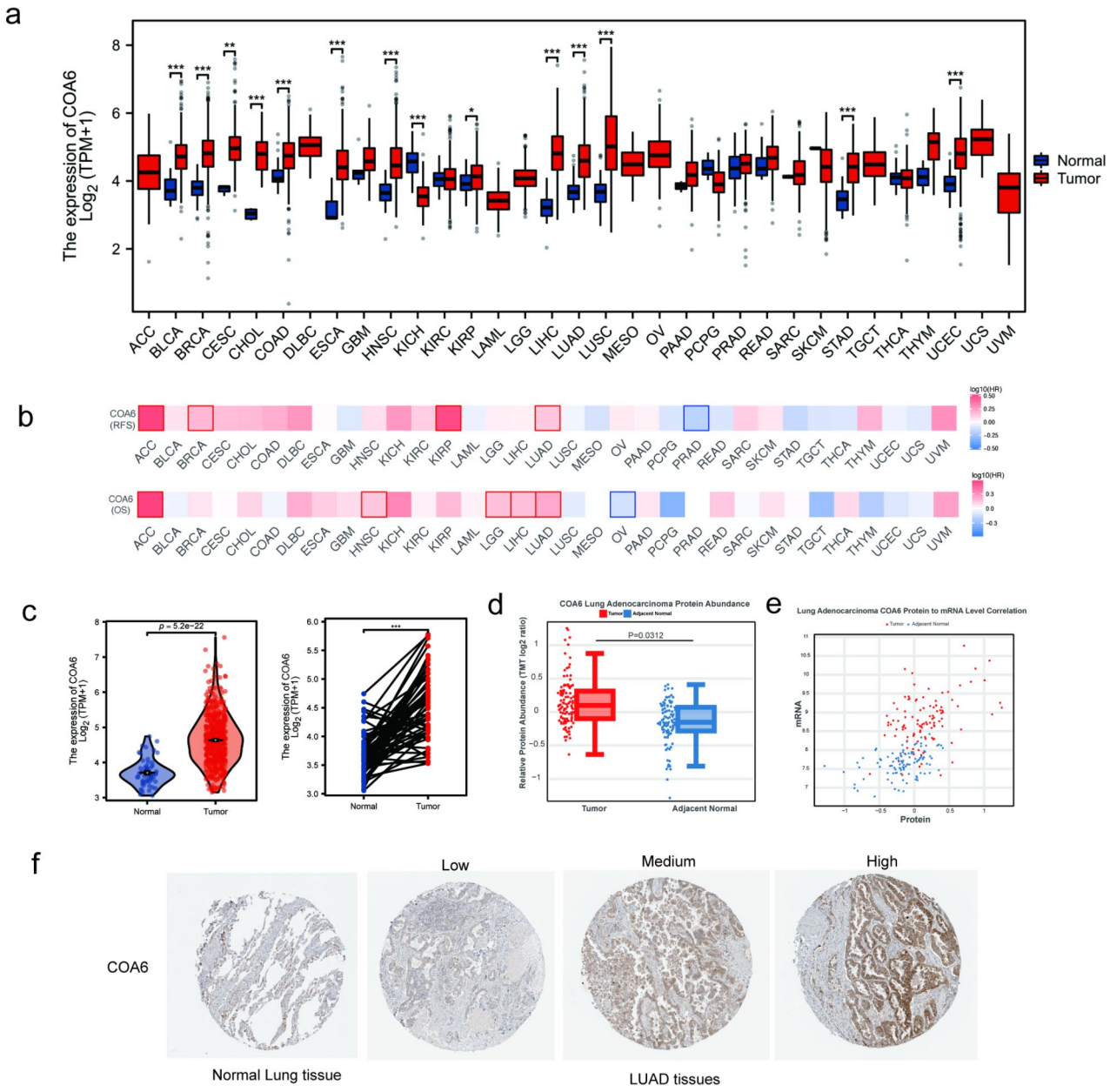

Fig. 1. Overexpression of COA6 in tumor tissues and its prognostic value across cancers. (**a**) The mRNA expression of COA6 in 33 types of tumor tissues and normal tissues in TCGA datasets. (**b**) Relationship between the expression of COA6 and overall survival /Disease Free Survival across cancers based on TCGA data. (**c**) The mRNA expression of COA6 between LUAD and normal tissues. (**d**) Protein expression of COA6 in LUAD samples in comparison to that in healthy tissue samples from the cProSite database. (**e**) The correlation between COA6 mRNA and protein abundance. (**f**) IHC images of COA6 protein in LUAD obtained from HPA database.

carcinoma(ACC), HNSC, brain lower grade glioma(LGG), and LIHC was correlated with poor OS, and COA6 upregulation was also associated with reduced recurrence free survival (RFS) in ACC, BRCA, kidney renal papillary cell carcinoma (KIRP), and LUAD (Fig. 1b). At the mRNA level, COA6 expression was significantly higher in LUAD than in normal lung tissues (Fig. 1c). Consistently, we found that the expression of COA6 at protein level in LUAD tissues was significantly higher than that in adjacent normal tissues (Fig. 1d) and was strongly positive correlated with that at mRNA level (cor = 0.55) (Fig. 1e). Figure 1f showed the COA6 histochemical staining picture of LUAD patients from HPA database. The cytoplasmic brown-yellow staining is evident, while the nucleus is blue, indicating that COA6 protein is distributed in the cytoplasm.

Correlations between COA6 expression and clinicopathological features

The baseline clinical characteristics of LUAD patients with different COA6 expression from TCGA database were showed in Supplementary Table 2. The expression of COA6 tended to be higher in more advanced pathologic stage in LUAD based on TCGA dataset, such as later T stage ($P=0.03$), positive lymph node metastasis ($P=0.02$) and positive distant metastasis ($P=0.03$) (Fig. 2a-d). In addition, we could see that COA6 expression was significantly lower in patients with disease control (SD + CR + PR) than in patients with progressive disease (PD) ($P=0.00019$) (Fig. 2e). There were no significant differences in COA6 expression between gender, race, age and smoking history (Fig. 2f). The ROC curve showed that COA6 had a highly predictive value (AUC = 0.882) in diagnosing LUAD from healthy lung tissues (Fig. 2g). Furthermore, the LUAD patients with high COA6 expression had shorter overall survival time (OS) than those with low COA6 expression in both the TCGA ($P<0.001$) and GSE31210 ($P=0.002$) datasets (Fig. 2h,i). Importantly, patients with high COA6 expression had significantly shorter OS in different clinical subgroups, including clinical stage, T stage, N stage, and different age groups (Supplementary Fig. S1a-g).

COA6 was an independent prognostic biomarker for OS in LUAD patients

According to the results from univariate and multivariate Cox regression analyses, COA6 was an independently variable for predicting OS in LUAD (Supplementary Tables 3 and Supplementary Table 4). We established a prognostic nomogram by integrating COA6 expression and TNM stage (Fig. 3a). The ROC curves indicated that our nomogram demonstrated a good predictive ability in predicting 1-year, 3-year, and 5-year OS of patients with LUAD in both the training (TCGA cohort) and testing sets (GSE31210) (Fig. 3b).

COA6 expression indicated high tumor mutational burden

Patients with high COA6 expression tended to obtain higher TMB values than those with low expression (Supplementary Fig. S2a). Besides, COA6 expression had a positive correlation with the tumor mutational burden (TMB) value ($R=0.22$, $P<0.001$) (Supplementary Fig. S2b). Displayed in the Supplementary Fig. S2c and S2d were the top 20 genes with highest mutation rate in COA6 low and high expression groups. TP53 (49%),

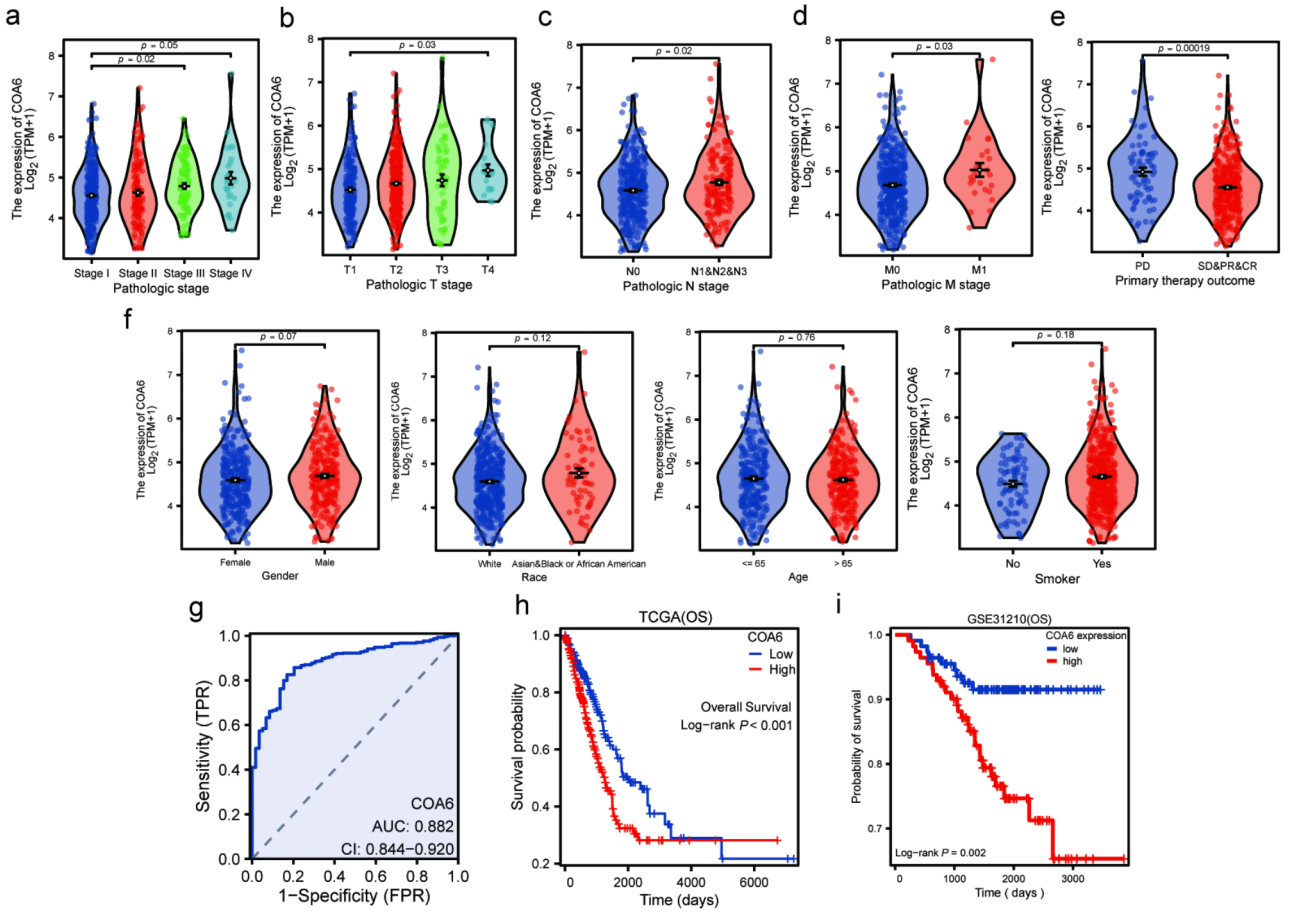

Fig. 2. Clinicopathological characteristics and prognostic value of COA6 in LUAD. (**a**–**f**) COA6 expression in different pathologic stage, T stage, N stage, M stage, primary therapy outcome, gender, race, age and smoking history of LUAD based on TCGA data. (**g**) ROC curve shows the diagnostic accuracy of COA6. (**h**,**i**) Kaplan-Meier survival curves for high and low COA6 expression groups are shown based on TCGA and GSE31210 datasets.

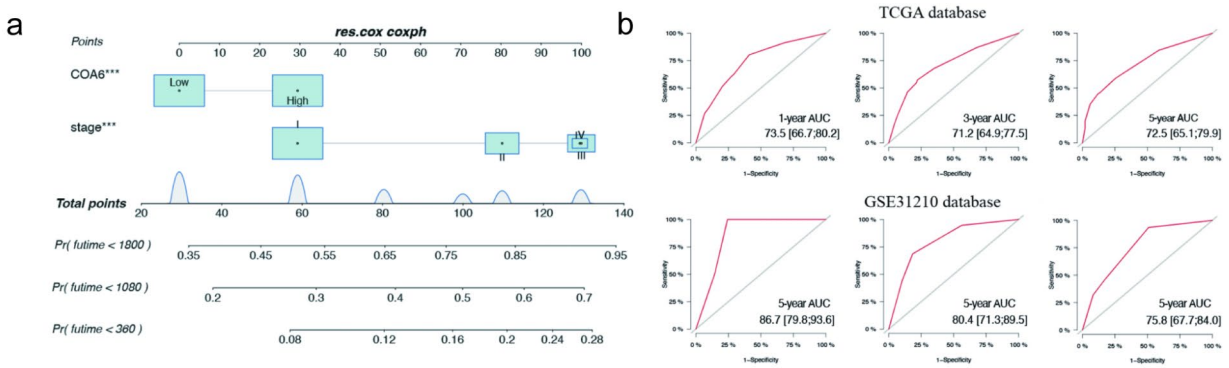

Fig. 3. The prognosis values of COA6 in LUAD patients. (**a**) Prognostic nomogram for LUAD based on TNM stage and COA6 expression level. (**b**) ROC curve analyses combined with TNM stage and COA6 expression for prognosis generated from TCGA database and GSE31210 datase.

genes such as TTN (47%), and RYR2 (40%) often mutated with low COA6 expression, while TP53 (47%), TTN (40%), and MUC16 (39%) were of high COA6 expression.

COA6 was involved in regulating the immune response in LUAD

We identified 303 differentially expressed genes between low and high COA6 expression groups and GO and KEGG analysis were conducted. As shown in Fig. 4a, we found that COA6 was associated with biological processes of humoral immune response, immunoglobulin mediated immune response and complement activation. The top 3 cellular components were immunoglobulin complex, external side of plasma membrane and collagen−containing extracellular matrix. Molecular functions of COA6 were mainly involved in immunoglobulin receptor binding, antigen binding and extracellular matrix structural constituent. For KEGG terms, Glutathione metabolism, ECM-receptor interaction, cell cycle and cell adhesion molecules were involved (Fig. 4b). Gene Set Enrichment Analysis (GSEA) showed that biological processes such as vascular smooth muscle contraction, JAK-STAT signaling pathway, and chemokine signaling pathway were conspicuously enriched in patients with low COA6 expression (Fig. 4c). In addition, we found that COA6 was involved in leukocyte trans-endothelial migration and Th17 cell differentiation. Furthermore, we screened 212 genes that significantly correlated with COA6 expression, including SNRPE($R=0.65$), HSPE1($R=0.63$), SNRPG($R=0.63$), and PSMD14 ($R=0.60$) etc. Protein-protein interaction (PPI) network for COA6 was visualized using STRING (https://cn.string-db.org/) and NEDD8 was determined as hub gene (Fig. 4d). Biological functions of those highly connected genes mainly included oxidoreductase complex, proteasome and respiratory chain complex IV (Fig. 4e).

We examined the expression of COA6 in the tumor microenvironment by analyzing single-cell sequencing data from two LUAD patients[21] (Fig. 5a). t-SNE plot indicated COA6 expression heterogeneity in different cell clusters (Fig. 5b). The correlation analysis between COA6 expression and cell functional states showed that the expression level of COA6 was positively related to cell cycle, invasion and negatively related to inflammation of LUAD cells (Fig. 5c, d). All of these indicated that COA6 was an oncogenic gene in LUAD and may involve in the regulation of the immune response.

COA6 shaped suppressive tumor immune microenvironment

Patients with high COA6 expression were characterized by lower stromal score, immune score, ESTIMATE score, and higher tumor purity (Fig. 6a-d), which suggested the lower infiltration of stromal cells and immune cell, and the high proportion of tumor cells in the tumor tissues of patients with high COA6 expression. Then, we analyzed association of 24 immune cells infiltration and COA6 expression. We can see that expression levels of COA6 significantly negatively correlated with natural killer (NK) cells, follicular helper T cell (TFH), effective memory T cell (Tem), eosinophils, interdigitating dendritic cells (iDC), central memory T cell (Tcm), B cells, mast cells, dendritic cell (DC), macrophages, T cells, plasmacytoid dendritic cells (pDC), Th1 cells, while positively correlated with Th2 cells, Gamma delta T cells (Tgd) infiltration in LUAD (Fig. 6e-h). Generally, high expression levels of COA6 correlated with decreased immune cells infiltration. To better understand tumor immune microenvironment in high COA6 expression patients, we further evaluated the relation between COA6 and immune checkpoints. We noted that high expression of COA6 in lung adenocarcinoma was accompanied by low expression of 14 out of 23 immune checkpoints, including TGFB1, CD274, CTLA4, and TIGIT (Fig. 6i). We evaluated the association between COA6 expression and the efficacy of immunotherapy in patients with LUAD. High COA6 expression indicated higher immune exclusion response but lower immune dysfunction response in the LUAD tumor microenvironment (Fig. 6j). However, no significant difference was observed in TIDE score between low and high COA6 expression groups, which implied patients with different expression level of COA6 may have comparable response to immunotherapy (Fig. 6j). Taken together, COA6 reshaped a suppressive tumor immune microenvironment in LUAD.

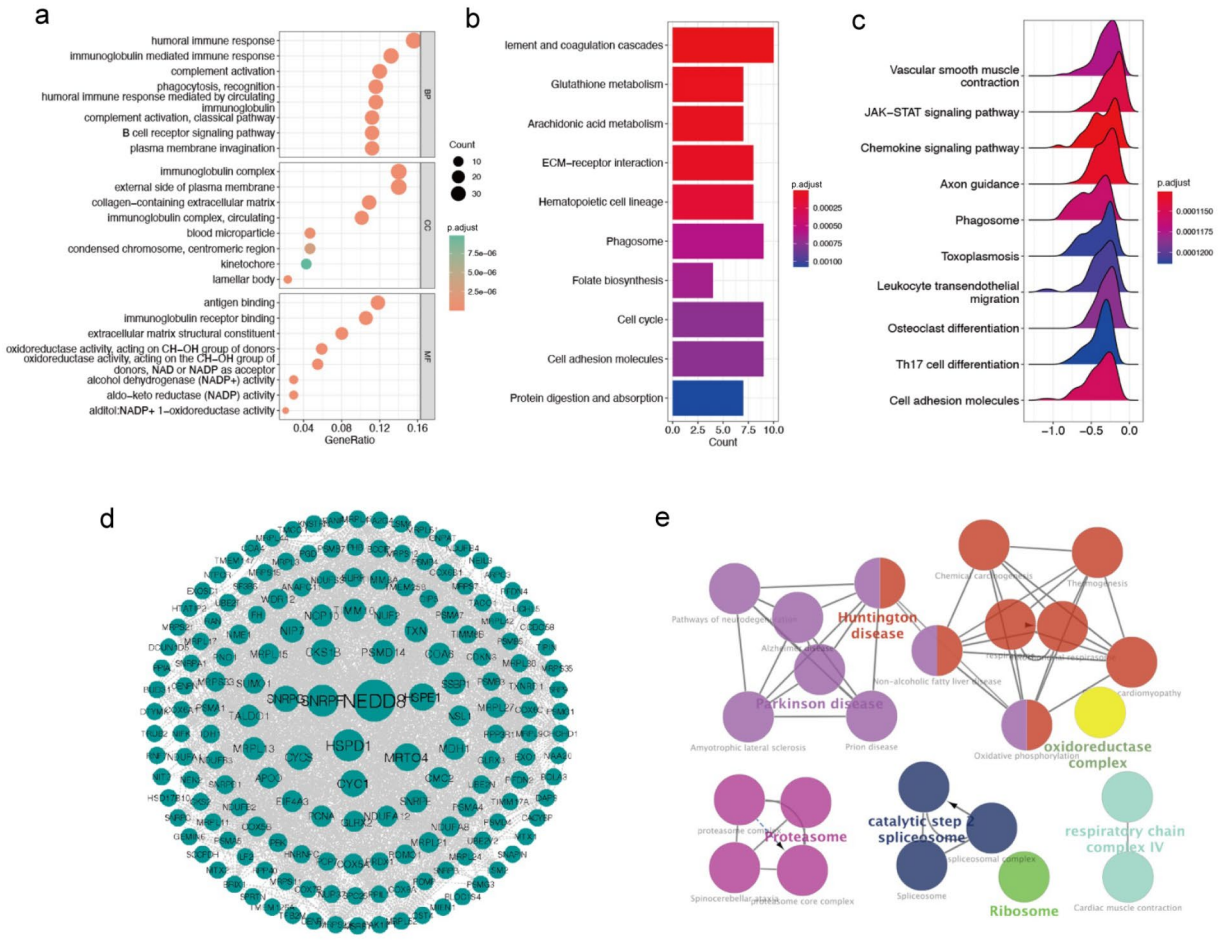

Fig. 4. Functional enrichment analysis and interaction network of COA6 in LUAD. (**a**,**b**) Top 8 significant GO terms and top 10 KEGG terms of 303 differentially expressed genes between COA6 low and high expression samples. (**c**) GSEA of differential expression genes in low and high expression COA6 groups in LUAD. (**d**) PPI network of 212 genes most positively associated with COA6. (**e**) Functional annotation analysis of the 212 genes based on the PPI network.

COA6 expression indicated the efficacy of antitumor drugs

We further evaluated the efficacy of multiple chemotherapeutic drugs in LUAD patients. Patients with high expression of COA6 tended to have a higher sensitivity to drugs such as gemcitabine (P=2e-07), etoposide (P=2.5e-07), doxorubicin (P=3.5e-05), and cisplatin (P=0.0025) (Supplementary Fig. S3a). As for targeted drugs, high COA6 expression patients were more sensitive to imatinib (P=6.5e-08), but less sensitive to sunitinib (p=2e-07), crizotinib (P=3.8e-05), and saracatinib (P=0.00095) (Supplementary Fig. S3b). Besides, we observed a good correlation between the expression of COA6 and the IC50 of these drugs (Supplementary Fig. S3c,d).

Validation of COA6 expression and function in LUAD

We found that COA6 expression in lung adenocarcinoma cell lines H1299, PC-9, H1975, and A549 was up-regulated to different degrees compared with in human normal lung epithelial cell line Beas-2B by RT-qPCR and western blot (Fig. 7a, b). Moreover, we performed COA6 IHC staining on paraffin sections of surgical LUAD and adjacent normal lung tissues. Typical images of different staining intensities of COA6 were shown in Fig. 7c. The staining score in LUAD tissues was higher compared with normal tissues.

We initially explored the role of COA6 in LUAD experimentally. To knock down COA6, we used lentivirus to infect with PC-9 and A549. Figure 8a and b demonstrated that we successfully knocked down COA6 at the mRNA and protein levels. Additional, MTT assay and clonal formation assay showed that the knockdown of COA6 weakened the proliferation ability and clonal formation ability of LUAD cells (Fig. 8c, d). A flow cytometry analysis showed that the COA6 knockdown cells were blocked in the G1 phase of the cell cycle (Fig. 8e).

To further clarify the role of COA6 in LUAD. We investigated the prognostic value and expression of COA6-related genes in LUAD. Based on the TCGA database, we found that high expression of NEDD8, PSMD14, SNRPE

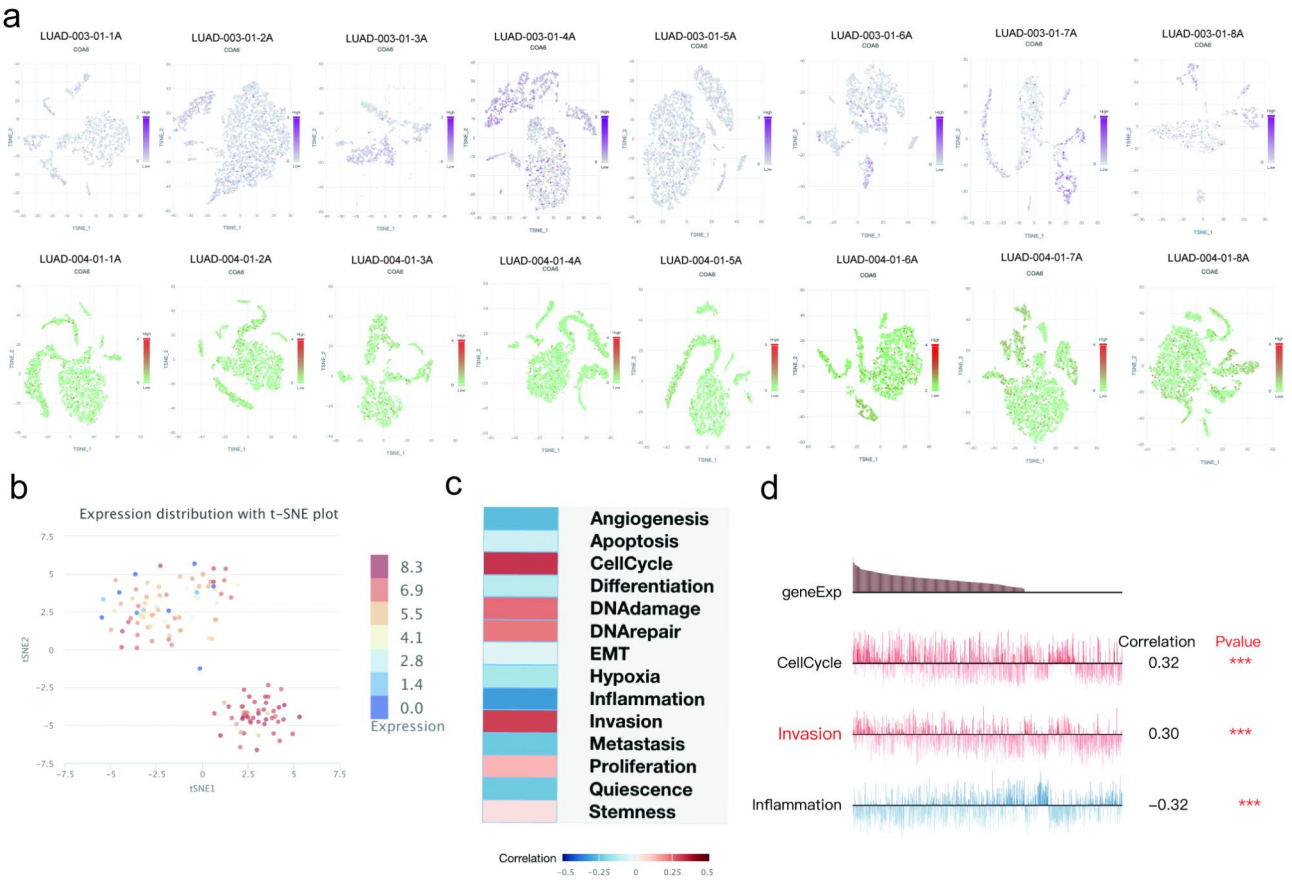

Fig. 5. COA6 expression distribution and related functional states in single-cell datasets. (**a**) t-SNE plot of different COA6 expression on immune cells from LUAD-003 and LUAD-004(001–008 A)patients. (**b**) Expression distribution of COA6 identified by single cell mRNA sequencing using a patient-derived xenograft LUAD samples (EXP0066). Every point represents a single cell, and the color of the point represents the expression level of COA6. (**c**,**d**) Correlations between COA6 and functional states in non-small cell lung cancer single-cell datasets (EXP0068). t-SNE: t-Distributed Stochastic Neighbor Embedding.

and HSPE1 were all associated with poor prognosis in LUAD patients (Supplementary Fig. S4a). Then, we found only PSMD14 expression was both inhibited in A549 and PC9 cells after COA6 knockdown (Supplementary Fig. S4b,c). Our single-cell sequencing analysis showed that COA6 expression was closely related to DNA damage repair signaling pathway, so we detected genes related to this pathway. The results suggested that silencing COA6 could inhibit the expression of ATR, ATM, CHEK1 and CHEK2 (Supplementary Fig. S4d,e).

Discussion

Tumor growth requires a large amount of energy supply, of which oxidative phosphorylation accounts for a large part. Therefore, targeting the metabolic vulnerability of cancer cells is becoming a new direction for the development of anti-tumor drugs. We focused on COA6, a necessary assembly factor, which takes part in COX biogenesis[22]. Firstly, we found that COA6 was upregulated in multiple cancer types, including LUAD. As a cancer-promoting gene, COA6 was a significant risk factor for the prognosis of patients with ACC, BRCA, KIRP, LUAD, etc., especially in LUAD, where high expression of COA6 was significantly negatively correlated with OS and RFS. Then, we evaluated the prognostic value of COA6 in different LUAD datasets, and found that COA6 was significantly correlated with later tumor stage and poor prognosis. In addition, it is interesting to note that there were varying degrees of mutations in a large number of genes such as TP53, TTN, and RYR2 in the two groups of LUAD patients with high and low expression of COA6, which can also explain the poor prognosis associated with high expression of COA6. Functionally, COA6 is related to LUAD cell proliferation and invasion. We found that the differentially expressed genes between the high and low expression groups of COA6, such as NEDD8, PSMD14, HSPE1, SNRPE, were enriched in the cell cycle, neddylation and DNA damage pathways. We also verified that COA6 knockout significantly inhibited the proliferation of LUAD cells and the G1 phase cell cycle arrest by flow cytometry and colony formation. In addition to participating in the process of mitochondrial respiratory, COA6 may also be involved in the process of antigen binding, immunoglobulin receptor binding. Meanwhile, we investigated the potential role of COA6 in immune infiltration. The high expression of COA6

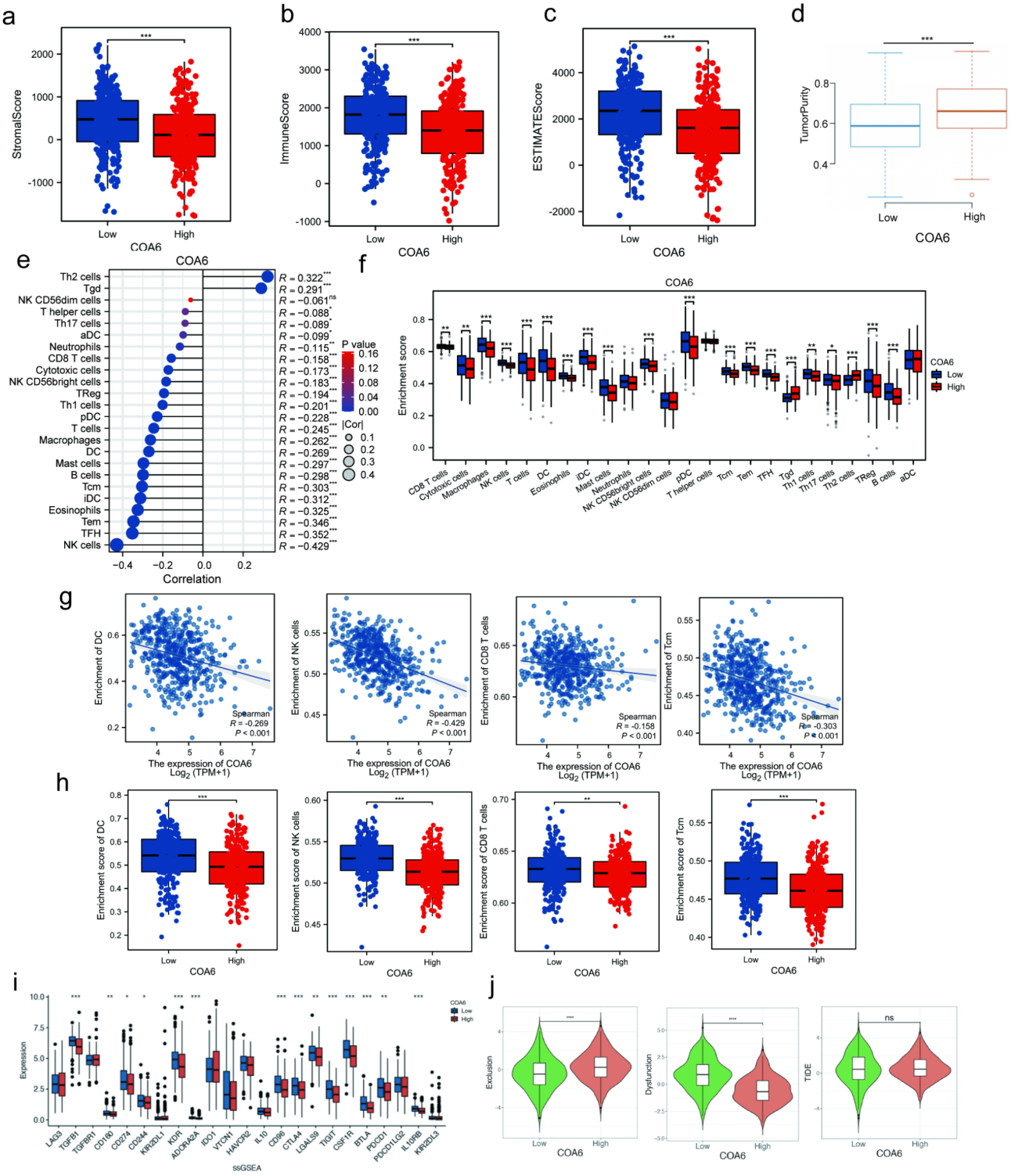

Fig. 6. Correlation analysis of COA6 expression with the immune-related signatures. (**a**–**d**) Stroma score, immune score, estimate score and tumor purity comparing in COA6 low and high groups. (**e**,**f**) Correlation between COA6 expression level and immune cells in the LUAD microenvironment. (**g**) Correlation of COA6 expression with DC cells, NK cells, CD8 + T cells and Tcm cells. (**h**) Differences of DC cells, NK cells, CD8 + T cells and Tcm cells among different COA6 expression groups. (**i**) Relation between COA6 and 23 immune checkpoints. (**j**) Comparison of immunotherapy response biomarkers, including Tumor Immune Dysfunction and Exclusion (TIDE) score, T-cell dysfunction score and T-cell exclusion score, between different COA6 expression groups.

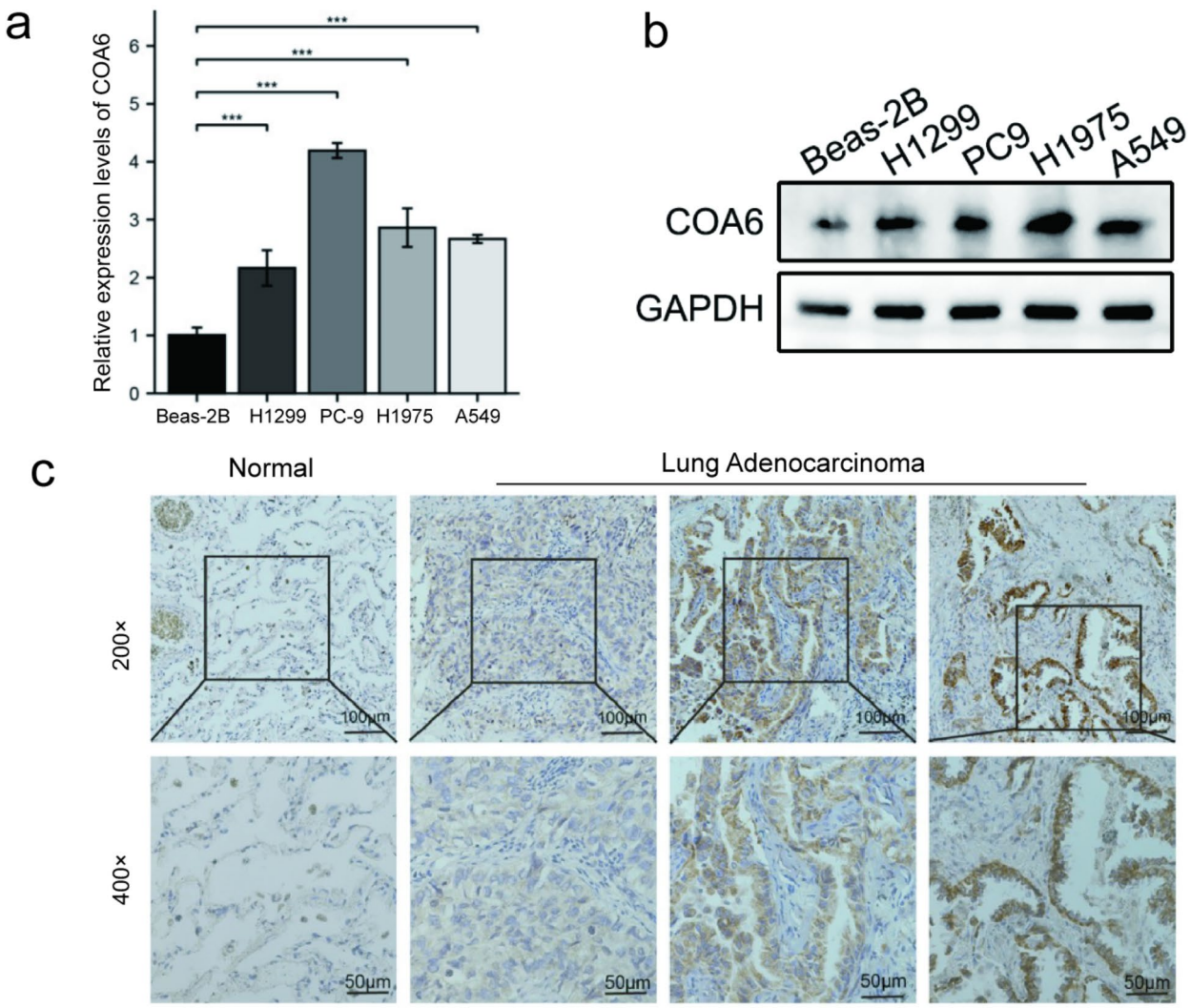

Fig. 7. COA6 expression in LUAD. (**a**, **b**) COA6 mRNA and protein expression in LUAD cell lines. (**c**) Immunohistochemical staining shows COA6 expression level in LUAD.

is related to the inhibitory immune microenvironment. The level of COA6 was positively correlated with TMB, and was associated with antitumor drugs' resistance, which may guide clinical decisions.

COA6 may play as an oncogene. Several studies demonstrated that COA6 is necessary for COX assembly while COX activity can be used to determine OXPHOS capacity[23]. In contrast to normal cell types, tumor cells display unimpaired OXPHOS[24]. We found that COA6 at both the mRNA and protein levels is significantly elevated in LUAD compared with normal lung cells. And COA6 related genes were enriched in OXPHOS gene set in LUAD, which suggested COA6 and OXPHOS were activated in LUAD. It is consistent with report of Zhang et al.[15]. However, the mechanism of how tumor cells upregulate COA6 still needs to be further explored.

COA6 may also serve as a potential drug target. Many types of cancer, or subpopulations of cancer cells including metastatic cells, therapy-resistant cells or cancer stem cells depend on mitochondrial OXPHOS, which suggests OXPHOS can serve as novel therapeutic targets in cancers[25–28]. Several studies implicate synergy of OXPHOS inhibitors with chemotherapy, targeted agents, angiogenesis inhibitors, glycolysis inhibitors and radiation in hypoxic tumors. For example, NSCLC with *Kras* and *Lkb1* mutations were selectively sensitive to phenformin, a complex I inhibitor[29]. LKB1 is a major upstream activator of AMPK which senses the energy status under energy stress. In the presence of decreased OXPHOS, tumor cells need to increase glycolytic to maintain ATP levels through AMPK regulation. Therefore, NSCLC with LKB1 deletion cannot fully upregulated glycolytic and exhibit sensitive to OXPHOS inhibitors[29]. Meanwhile, a study reported that after long term EFGR-TKI therapy, NSCLC appear to be more OXPHOS-dependent[30]. It suggests combination of EFGR-TKI and OXPHOS inhibitor could exert better efficacy on NSCLC. Another study suggested that As_2O_3 improved response to radiotherapy as a result of an increase tumor oxygenation[7]. We found that COA6 knockdown inhibited LUAD cell proliferation. High COA6 expression patients were less sensitive to sunitinib, crizotinib, and saracatinib. So, targeting COA6 may combine with these drugs.

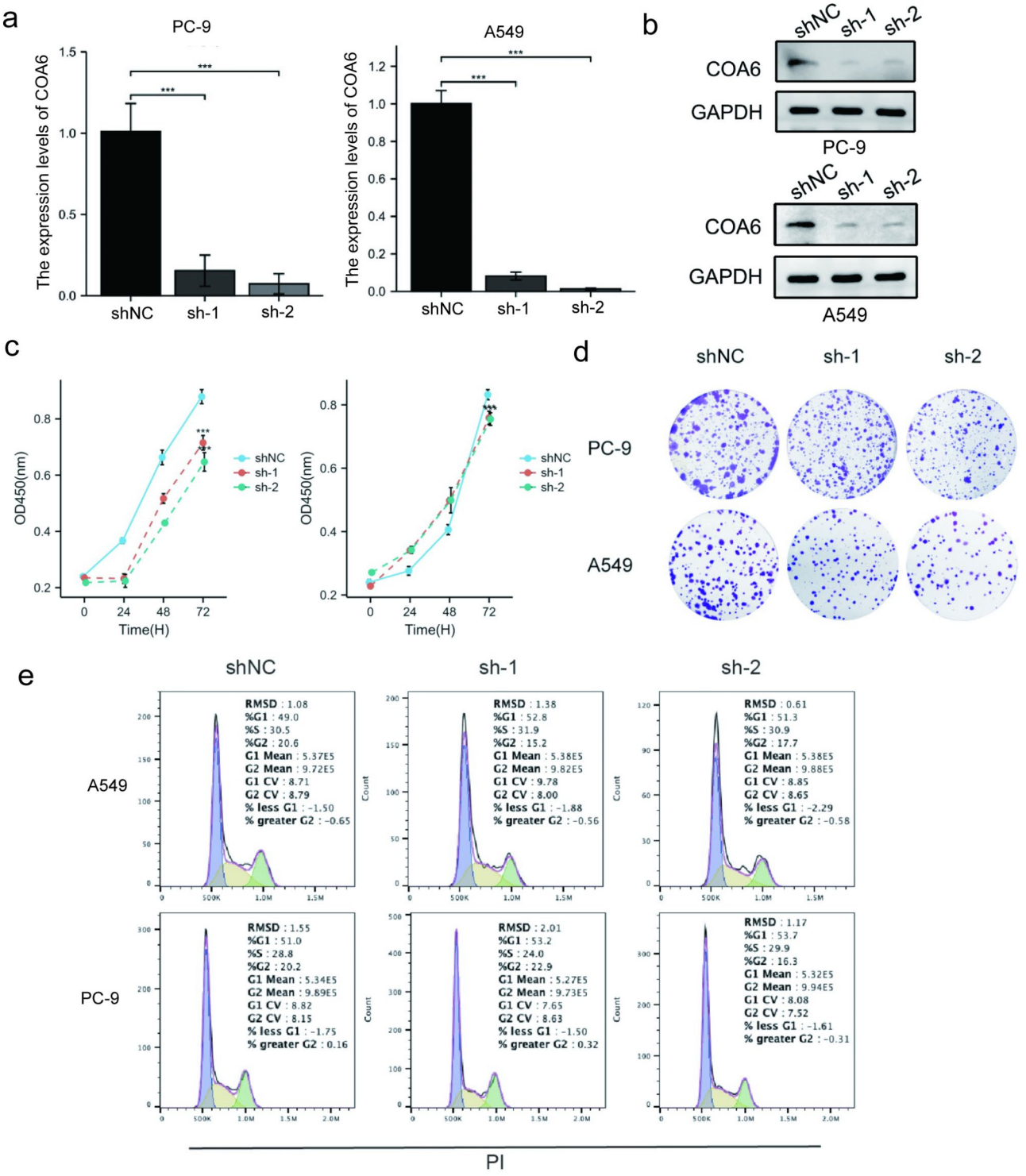

Fig. 8. COA6 function in LUAD. (**a**, **b**) COA6 shRNA transfection efficiency was validated by RT-qPCR and western blot. (**c**, **d**) The cell proliferative ability was detected by MTT assay and cell clone formation assay with COA6 knockdown (sh-1, sh-2) or negative control (shNC) in LUAD cell lines. (**e**) Cytoflow-based cell cycle analysis of COA6 knockdown and negative control LAUD cells.

High expression of COA6 in LUAD is associated with poor prognosis. We considered that not only a result of tumor cell proliferation enhanced by OXPHOS but also a result of anticancer TME suppression. The prominent TME components are infiltrating stromal cells and immune cells, which can affect tumor progression[31]. Our study showed that the high COA6 expression LUAD group had significantly higher tumor purity, lower stromal cells and lower immune cells when compared with the low COA6 expression group. High COA6 expression are

associated with decreased infiltration of most types of immune cells. This partly explains relatively low level of immune checkpoints in COA6 high expression group. Notably, increased Th2 cells significantly associated with high COA6 expression. Cytokine production from Th2 cells inhibits proliferation and differentiation of Th1 cells and cytotoxic T lymphocytes[32], which results in immunosuppressive effects on tumor and tumor immune escape. Single cell sequencing analysis demonstrated that COA6 expression were negatively correlated with inflammation, which is consists with the immune cells analysis.

The main challenge of tumor immunotherapy is to modulate the suppressive tumor microenvironment to favor the elicitation of strong anti-tumor immune responses. Recent study has found that compared with the PD-1-sensitive model, PD-1-resistant model increased OXPHOS utilization significantly. OXPHOS inhibitors combined with radiotherapy can improve tumor immunity and reduce radiation-induced immunosuppression in PD-1 resistant NSCLC[33]. Therefore, targeting COA6 to reactivate the TME microenvironment may be a choice to enhance the efficacy of checkpoint inhibitors.

Our study has some limitations. First, we performed most of our analyses using data from the public databases. Clinical data is relatively insufficient. Secondly, the relationship between COA6 and tumor immune microenvironment still needs to be verified by in vivo experiments. Finally, we used LUAD cell lines to perform functional experiments, which simply demonstrated COA6 function in cancer cell proliferation. The specific mechanism still needs to be further investigated.

In conclusion, we found that COA6 was upregulated and promoted lung adenocarcinoma progression. Meanwhile, COA6 was associated with the suppressive tumor microenvironment. Thus, COA6 has the potential to serve as a prognostic biomarker or a new anticancer target in clinical practice.

Data availability

The datasets presented or analyzed during this study are freely available in the TCGA database (https://portal.gdc.cancer.gov/) and its supplementary information files. The authors declare that they take complete responsibility for the integrity of the data and the accuracy of the data analysis.

Received: 8 February 2024; Accepted: 25 October 2024
Published online: 29 October 2024

References

1. Zu, X. L. Cancer metabolism: facts, fantasy, and fiction. *Biochem. Biophys. Res. Commun.* **313**, 459–465 (2004).
2. Fernandez-Vizarra, E. et al. Assembly of the oxidative phosphorylation system in humans: what we have learned by studying its defects. *Biochim. Biophys. Acta* **1793**, 200–211 (2009).
3. Mick, D. U. et al. Inventory control: cytochrome c oxidase assembly regulates mitochondrial translation. *Nat. Rev. Mol. Cell. Biol.* **12**, 14–20 (2011).
4. Timón-Gómez, A. et al. Mitochondrial cytochrome c oxidase biogenesis: Recent developments. *Semin Cell. Dev. Biol.* **76**, 163–178 (2018).
5. Lee, J. et al. Effective breast cancer combination therapy targeting BACH1 and mitochondrial metabolism. *Nature* **568**, 254–258 (2019).
6. Wilk, A. et al. Molecular mechanisms of fenofibrate-induced metabolic catastrophe and glioblastoma cell death. *Mol. Cell. Biol.* **35**, 182–198 (2015).
7. Diepart, C. et al. Arsenic trioxide treatment decreases the oxygen consumption rate of tumor cells and radiosensitizes solid tumors. *Cancer Res.* **72**, 482–490 (2012).
8. Sung, H. et al. Global cancer statistics 2020: GLOBOCAN estimates of incidence and mortality worldwide for 36 cancers in 185 countries. *CA Cancer J. Clin.* **71**, 209–249 (2021).
9. Travis, W. D. et al. The 2015 World Health Organization classification of lung tumors: Impact of genetic, clinical and radiologic advances since the 2004 classification. *J. Thorac. Oncol.* **10**, 1243–1260 (2015).
10. Stroud, D. A. et al. COA6 is a mitochondrial complex IV assembly factor critical for biogenesis of mtDNA-encoded COX2. *Hum. Mol. Genet.* **24**, 5404–5415 (2015).
11. Ghosh, A. et al. Mitochondrial disease genes COA6, COX6B and SCO2 have overlapping roles in COX2 biogenesis. *Hum. Mol. Genet.* **25**, 660–671 (2016).
12. Baertling, F. et al. Mutations in COA6 cause cytochrome c oxidase deficiency and neonatal hypertrophic cardiomyopathy. *Hum. Mutat.* **36**, 34–38 (2015).
13. Calvo, S. E. et al. Molecular diagnosis of infantile mitochondrial disease with targeted next-generation sequencing. *Sci. Transl. Med.* **4**, 118ra110 (2012).
14. Han, S. et al. Cuproptosis-related genes CDK1 and COA6 involved in the prognosis prediction of liver hepatocellular carcinoma. *Dis. Mark.* 5552798 (2023).
15. Zhang, M. et al. High expression of COA6 is related to unfavorable prognosis and enhanced oxidative phosphorylation in lung adenocarcinoma. *Int. J. Mol. Sci.* **24** (2023).
16. Zhang, X. et al. A novel mitochondrial-related nuclear gene signature predicts overall survival of lung adenocarcinoma patients. *Front. Cell. Dev. Biol.* **9**, 740487 (2021).
17. Kanehisa, M. KEGG: Kyoto encyclopedia of genes and genomes. *Nucleic Acids Res.* **28**, 27–30 (2000).
18. Kanehisa, M. A. O. et al. KEGG for taxonomy-based analysis of pathways and genomes. *Nucleic Acids Res.* **51**, D587–D592 (2023).
19. Kanehisa, M. A. O. X. Toward understanding the origin and evolution of cellular organisms. *Protein Sci.* **28**, 1947–1951 (2019).
20. Bindea, G. et al. Spatiotemporal dynamics of intratumoral immune cells reveal the immune landscape in human cancer. *Immunity* **39**, 782–795 (2013).
21. Lambrechts, D. et al. Phenotype molding of stromal cells in the lung tumor microenvironment. *Nat. Med.* **24**, 1277–1289 (2018).
22. Papadopoulou, L. C. et al. Fatal infantile cardioencephalomyopathy with COX deficiency and mutations in SCO2, a COX assembly gene. *Nat. Genet.* **23**, 333–337 (1999).
23. Larsen, S. et al. Biomarkers of mitochondrial content in skeletal muscle of healthy young human subjects. *J. Physiol.* **590**, 3349–3360 (2012).
24. Vaupel, P. & Mayer, A. Availability, not respiratory capacity governs oxygen consumption of solid tumors. *Int. J. Biochem. Cell. Biol.* **44**, 1477–1481 (2012).
25. Lin, S. et al. The mitochondrial deoxyguanosine kinase is required for cancer cell stemness in lung adenocarcinoma. *EMBO Mol. Med.* **11**, e10849 (2019).
26. Iranmanesh, Y. et al. Mitochondria's role in the maintenance of cancer stem cells in glioblastoma. *Front. Oncol.* **11**, 582694 (2021).

27. Baccelli, I. et al. Mubritinib targets the electron transport chain complex I and reveals the landscape of OXPHOS dependency in acute myeloid leukemia. *Cancer Cell* **36**, 84–99e88 (2019).
28. Sotgia, F. et al. A mitochondrial based oncology platform for targeting cancer stem cells (CSCs): MITO-ONC-RX. *Cell Cycle* **17**, 2091–2100 (2018).
29. Shackelford, D. B. et al. LKB1 inactivation dictates therapeutic response of non-small cell lung cancer to the metabolism drug phenformin. *Cancer Cell* **23**, 143–158 (2013).
30. Kim, S. et al. Enhanced sensitivity of nonsmall cell lung cancer with acquired resistance to epidermal growth factor receptor-tyrosine kinase inhibitors to phenformin: the roles of a metabolic shift to oxidative phosphorylation and redox balance. *Oxid Med Cell Longev.* 5428364 (2021).
31. Goenka, A. et al. Tumor microenvironment signaling and therapeutics in cancer progression. *Cancer Commun. (Lond.)* **43**, 525–561 (2023).
32. Guenova, E. et al. TH2 cytokines from malignant cells suppress TH1 responses and enforce a global TH2 bias in leukemic cutaneous T-cell lymphoma. *Clin. Cancer Res.* **19**, 3755–3763 (2013).
33. Chen, D. et al. Combination treatment with radiotherapy and a novel oxidative phosphorylation inhibitor overcomes PD-1 resistance and enhances antitumor immunity. *J. Immunother Cancer* **8** (2020).

Author contributions

L.W. participated in study design, data analysis and drafted the manuscript. J.Y. and L.G. performed the data analysis and contributed to visualization. H.D. and Q.T. contributed for overall editing and supervision. All authors reviewed the manuscript.

Funding

This work was supported by grants from National Nature Science Foundation of China (Grant No.82172635 and No.82272686). This work was supported by Cancer Biobank of Tianjin Medical University Cancer Institute & Hospital.

Declarations

Competing interests

The authors declare no competing interests.

Additional information

Supplementary Information The online version contains supplementary material available at https://doi.org/10.1038/s41598-024-77775-y.

Correspondence and requests for materials should be addressed to D.H. or T.Q.